Contents

List of Contributors

Veronica Angelica Villalobos Romo
Universidad Autonoma de Ciudad Juarez, 450 north Av. Del Charro, Ciudad Juarez, Chih. 32310, Mexico, e-mail: veronica.villalobos@uacj.mx

Soledad Vianey Torres Arguelles
Universidad Autonoma de Ciudad Juarez, 450 north Av. Del Charro, Ciudad Juarez, Chih. 32310, Mexico, e-mail: vianey.torre@uacj.mx

Claudia Georgina Nava Dino
Universidad Autónoma de Chihuahua, Circuito Universitario 2, Chihuahua, Chih. 31125, Mexico, e-mail: vianey.torre@uacj.mx

Jose Manuel Mejia Muñoz
Universidad Autonoma de Ciudad Juarez, 450 north Av. Del Charro, Ciudad Juarez, Chih. 32310, Mexico, e-mail: jose.mejia@uacj.mx

Edgar Daniel Gomez García
Universidad Autonoma de Ciudad Juarez, 450 north Av. Del Charro, Ciudad Juarez, Chih. 32310, Mexico, e-mail: edgardanielgomez.18@gmail.com

Corresponding: José David Diaz Román
Universidad Autonoma de Ciudad Juarez, 450 north Av. Del Charro, Ciudad Juarez, Chih. 32310, Mexico, e-mail: david.roman@uacj.com

Chapter 1
Decision Support System in Smart Healthcare: System for diagnosis of skin cancer using deep learning

Veronica Angelica Villalobos Romo[0000−0002−8021−5145] and
Soledad Vianey Torres Arguelles[0000−0003−0978−3796] and
Claudia Georgina Nava Dino[0000−0002−8714−3690] and
Jose Manuel Mejia Muñoz[0000−0002−5832−6623] and
Edgar Daniel Gomez Garcia[NOTIENEORCID] and
Jose David Diaz Roman[0000−0002−8246−6562]

Abstract This chapter presents a mobile application as a decision support system for detecting six types of pigmented skin lesions using deep learning. Melanoma, the most aggressive of these conditions, represents only 1% of skin cancer cases but causes most deaths. Early detection is crucial for a higher chance of cure. In low-income countries, insufficient equipment and specialists make early diagnosis challenging. This mobile application aims to address the problem by allowing non-specialists to make a probable early detection of skin cancer and thus make the decision to consult a medical specialist. The decision support system uses convolutional neural networks with dense layers and applies the SMOTE [1] method to balance the dataset. Evaluations using the HAM10000 and PAD-UFES databases show a classification accuracy of over 80% across six skin cancer classes, with an

Veronica Angelica Villalobos Romo
Universidad Autonoma de Ciudad Juarez, 450 north Av. Del Charro, Ciudad Juarez, Chih. 32310, Mexico, e-mail: veronica.villalobos@uacj.mx

Soledad Vianey Torres Arguelles
Universidad Autonoma de Ciudad Juarez, 450 north Av. Del Charro, Ciudad Juarez, Chih. 32310, Mexico, e-mail: vianey.torre@uacj.mx

Claudia Georgina Nava Dino
Universidad Autónoma de Chihuahua, Circuito Universitario 2, Chihuahua, Chih. 31125, Mexico, e-mail: vianey.torre@uacj.mx

Jose Manuel Mejia Muñoz
Universidad Autonoma de Ciudad Juarez, 450 north Av. Del Charro, Ciudad Juarez, Chih. 32310, Mexico, e-mail: jose.mejia@uacj.mx

Edgar Daniel Gomez García
Universidad Autonoma de Ciudad Juarez, 450 north Av. Del Charro, Ciudad Juarez, Chih. 32310, Mexico, e-mail: edgardanielgomez.18@gmail.com

Corresponding: José David Diaz Román
Universidad Autonoma de Ciudad Juarez, 450 north Av. Del Charro, Ciudad Juarez, Chih. 32310, Mexico, e-mail: david.roman@uacj.com

improvement of up to 9% when SMOTE is applied. The lightweight application (284 MB) processes images directly from the smartphone camera or stored images, achieving a latency of 9.33 seconds per response. This allows the processing of six patients per minute and 360 patients per hour. The proposed system offers significant potential to improve early diagnosis and treatment of skin cancer, particularly in resource-limited settings.

1.1 Introduction

Skin cancer has become a global public health issue, with its incidence increasing over the past decades [2, 3]. The morphological characteristics of skin lesions are crucial factors in the diagnosis and early detection of cancer [4]. The skin, the largest organ of the human body, covers between 1.5 and 2 square meters and weighs approximately 4.2 kg [3]. The term "skin cancer" encompasses several neoplasms that share malignant behavior; however, individually they show very diverse degrees of local aggressiveness, tendency to metastasize, and mortality. These differences in malignancy are one of the most distinctive characteristics of skin cancer. The least malignant skin cancer, basal cell carcinoma, develops in the skin, as does one of the most aggressive neoplasms, melanoma. There can be superficial, slow-growing carcinomas to highly destructive invasive tumors capable of metastasizing [2, 3, 4].

The American Cancer Society estimates that approximately 100,350 new cases of melanoma will be diagnosed in the U.S. (about 60,190 men and 40,160 women). Melanoma is considered rare in Mexico, with an incidence of less than one case per 100,000 inhabitants, representing around 2,700 cases annually [5]. However, identifying melanoma is crucial as it has been detected that those susceptible to skin cancer in Mexico include farmers, sailors, street vendors, and individuals with genetic predispositions. Most of these people can be considered low-income, leading to a lower likelihood of early diagnosis and timely treatment [5, 6, 7]. In developing countries like Mexico and Brazil, particularly in peripheral areas, there is a lack of dermatologists and dermatoscopy equipment. Mobile devices can be a useful tool in this situation, given the high number of mobile subscriptions; according to Kassianos et al. [8], there were nearly eight billion subscriptions in 2019.

Numerous works have been proposed for melanoma detection using convolutional neural networks (CNN) on dermoscopic images. However, data imbalance in the available datasets has been a recurring problem, as the classification categories are not equally represented [9, 10]. In the medical field, a significant numerical imbalance in the number of samples of different lesion classes is common [11, 12]. In this context, machine learning has emerged as a powerful tool for medical image classification and disease detection [13, 14, 15, 16].

For example, Dai X. et al. [17] developed a classifier using the HAM10000 database [18], achieving an accuracy of 70%. On the other hand, Castro P. et al. [19] employed the MUPEB balancing technique (Extra-Polarization and Differential

Evolution Balancing) with the PAD-UFES database [20], achieving an accuracy of 83%. This result represented a 6% and 16% increase in accuracy and sensitivity, respectively, compared to previous works.

Data imbalance remains a significant challenge in developing effective classification methods. In 2019, R. Gao et al. evaluated the use of the Synthetic Minority Over-sampling Technique (SMOTE) in classifying facial skin pigmentation disorders, confirming a 7% improvement in accuracy for the two classes with the fewest data points [21, 1].

In [22], the SMOTE technique was implemented on imbalanced data from the HAM10000 skin cancer image repositories. Subsequently, a convolutional neural network-based architecture was used to classify seven classes of skin lesions. This approach has the potential to significantly improve accuracy and sensitivity in detecting melanoma and other skin lesions, thereby contributing to earlier and more effective skin cancer diagnosis [22]. It is estimated that in 2022, there were 335,000 new cases of melanoma worldwide, and around 60,000 people died from the disease [23].

1.1.1 Importance of Artificial Intelligence and Data Analytics in Medical Imaging

In the health sector, artificial intelligence, data analytics, and image processing are fundamental for decision-making, diagnosing, and treating various diseases, representing the most innovative advancements. Through data analysis and advanced technology, it is now possible to detect diseases, initiate immediate treatment, and increase the chances of success [24]. Modern algorithms assist doctors in utilizing everything from MRI images to laboratory test results to identify patterns and signals that may indicate the presence of a disease. In this way, data analytics facilitates the analysis of large volumes of medical data to improve patient care and medical research [24, 25, 26]. Medical image processing and data analytics enable healthcare professionals to make more precise and personalized diagnoses. According to a study by Saba et al. (2019), the use of deep learning algorithms in medical imaging has significantly improved the ability to detect diseases such as breast cancer and melanoma [25]. Therefore, data analytics helps manage large amounts of data into clear and useful information. This allows for more informed decision-making with less risk, as they are based on concrete data. Additionally, leveraging the potential massive amounts of data in the medical field ensures that care is appropriate for the patient and delivered at the right time, being potentially beneficial for everyone involved in the healthcare sector [27]. Artificial intelligence and data analysis are related, although they have different goals and objectives. Artificial intelligence aims to create autonomous and intelligent systems, while data analysis focuses on extracting valuable information from data to support decision-making. Both are

important in the information age and are constantly evolving, providing opportunities for development and research in various areas such as the health sector [27].

1.1.2 Skin Cancer and Its Diagnosis

The detection and diagnosis of skin cancer have traditionally been carried out through visual inspection combined with a systematic evaluation or examination process to identify the disease. However, this depends on the dermatologist's experience, making the processes lengthy, subjective, and possibly prone to errors [28]. This is due to the complex nature of skin lesions. Additionally, diagnosing skin cancer is not just about identifying melanoma or non-melanoma. It also includes multiple skin lesions, which complicates specialized analyses, such as distinguishing a melanocytic nevus from a melanoma or from basal cell carcinoma and squamous cell carcinoma, among other lesions [7]. Consequently, Computer-Aided Diagnosis (CAD) systems become necessary for the preliminary diagnosis of different lesions [29].

The use of deep learning technology with Convolutional Neural Networks (CNN) helps specialists identify and diagnose skin lesions, such as melanoma, more accurately and efficiently, leading to new research and developments to improve the performance of CAD in addressing many other complex clinical problems [29]. Using CAD with CNN provides a powerful tool that supports healthcare professionals in identifying skin lesions, improving diagnostic accuracy, and enabling earlier and more effective interventions. By combining medical expertise with advanced technology, more precise and efficient patient care is achieved [30].

Advances in smartphone cameras have enabled their potential use for the early detection of skin cancer. Smartphones can now recognize characteristics associated with skin cancer. To achieve this, Convolutional Neural Networks (CNNs) are commonly used for the detection and classification of diseases [31]. However, only a few deep learning models can be utilized to create a mobile application, as they require high computational power and large memory, which is challenging to implement on smartphones [32]. Nonetheless, various studies have developed mobile applications on smartphones with favorable results [30, 31, 32, 33].

Therefore, the development of a mobile application for skin cancer detection is essential, as it offers an accessible and portable tool for users to identify skin problems and seek timely medical attention. Additionally, the presence of a precise and easy-to-use diagnostic tool on a common device such as smartphones can significantly reduce the burden on healthcare systems, allowing professionals to provide appropriate treatment for the overall well-being of patients.

1.2 Methodology

This section describes the methodology used to create the application that detects skin cancer using images, First, image repositories with clinically diagnosed and classified cases by healthcare professionals were sought; then, the data were balanced with the SMOTE method, followed by the design of a dense network fully connected with convolutional adjustable base, where it was evaluated with convolutional architectures where two were of low weight and the remaining two were of high weight, these architectures were taken from the Keras library and a fine tuning was applied; then an application based on java language was designed to run on an Android device, and finally the system was simulated with test users to finally evaluate the effectiveness of the application. Figure 1.1 shows a diagram describing the process carried out in this methodology.

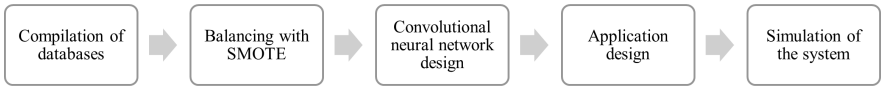

Fig. 1.1 Methodology process

Each section proposed in the methodology is detailed below.

1.2.1 Compilation of Databases

Training artificial neural networks to perform classification requires pre-labeled data, meaning each image must have a title or an attached file indicating the class or object contained in the image. For this reason, the HAM10000 database [18] was optimal for this project. This repository contains images of various types of skin diseases and syndromes, previously classified by healthcare professionals.
It consists of 10,015 dermatoscopic images with a uniform size of 1024x1024 in jpg format, which are publicly available. Table 1.1 shows the number of images for each of the classes included in the database.

On the other hand, images from the PAD-UFES repository [20] were also used, which contains clinical images of skin lesions properly labeled. The images were acquired with mobile devices and vary in size from 256x256 to 1024x1024 in PNG format. This dataset is an effort to assist researchers in developing low-budget tools, particularly to aid in skin cancer detection. Table 1.2 shows the number of images per class in the PAD-UFES database.

For this work, the vascular lesion class was first eliminated from the HAM10000 database because this classification is a skin lesion and not a pathology. Subsequently, both databases were concatenated in such a way that when adding all the images from PADUFES to HAM1000, 1165 images of melanoma, 1334 of benign keratosis,

Table 1.1 Distribution by class in HAM10000 Database.

Injury	Quantity
Melanocytic nevi (nv)	6705
Melanoma (mel)	1113
Benign keratosis (bkl)	1099
Basal cell carcinoma (bcc)	514
Actinic Keratoses (akiec)	327
Dermatofibroma (df)	142
Vascular skin lesions (vasc)	115

[a] HAM 10000

Table 1.2 Distribution by class in PAD-UFES Database.

Injury	Quantity
Melanocytic nevi (nv)	244
Melanoma (mel)	52
Benign keratosis (bkl)	235
Basal cell carcinoma (bcc)	845
Actinic Keratoses (akiec)	730
Dermatofibroma (df)	192

[a] PAD-UFES

1359 of basal carcinoma and 1057 of actinic keratosis were obtained; Since a similar number of images per class is sought, it was decided to use the 244 images of moles from the PADUFES and add them with a random sampling of 956 images from the HAM10000 to result in a final number of 1200 images of moles and thus have a balanced distribution among the above classes of lesions. As for the dermatofibroma class the sum of images from both databases resulted in 307 images. A random undersampling of the nv class was performed. Table 1.3 shows the distribution of images per class after combining both the HAM10000 and PAD-UFES databases.

Table 1.3 Distribution by Class When Combining Both Databases.

Injury	Quantity
Melanocytic nevi (nv)	1200
Melanoma (mel)	1165
Benign keratosis (bkl)	1334
Basal cell carcinoma (bcc)	1359
Actinic Keratoses (akiec)	1057
Dermatofibroma (df)	307

1.2.2 Balancing with SMOTE

The SMOTE data balancing technique was used only on the dermatofibroma class, because it was the class with the smallest number of images. For this purpose, first the images of two classes were separated in different folders, where in one of them there were the images of the minority class that needed to be balanced, i.e. ”squamous cancer” and in the other one there was a reference class with the number of images to be obtained at the end; the benign keratosis class was used for this purpose. Subsequently, the images of both classes were resized to a size of 256x256 pixels to have a standard measurement. This was done because both databases handle different sizes.
The processing of the data to perform the balancing by SMOTE [34] consisted of the following: the first step is to parameterize the values of each RGB (Red, Green and Blue) combination of the pixels of each image to bring these values to a two-dimensional plane, where each point in this plane represents an image. Next, a random point from the minority class and a random point from the reference class are selected and a new point is generated at half the distance between these two points. This process was repeated until the same amount of data (images) from the minority class was obtained with respect to the reference class. Figure 1.2 shows examples of the results of the false images generated with SMOTE.

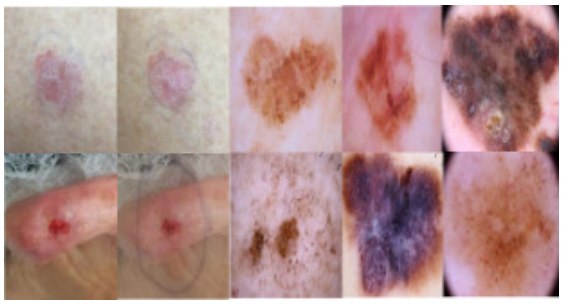

Fig. 1.2 Fake images generated with SMOTE of the dermatofibroma class

A total of 804 dermatofibroma images were generated and added to the total image set, resulting in the distribution shown in Figure 1.3.

The images were separated in a stratified way, where 20% of all images (not including the images artificially generated with SMOTE) were reserved from the beginning to test the performance of the model. To the remaining 80%, the artificial images were added, and from this total 80% were separated for network training and 20% for a validation set to be used during training.

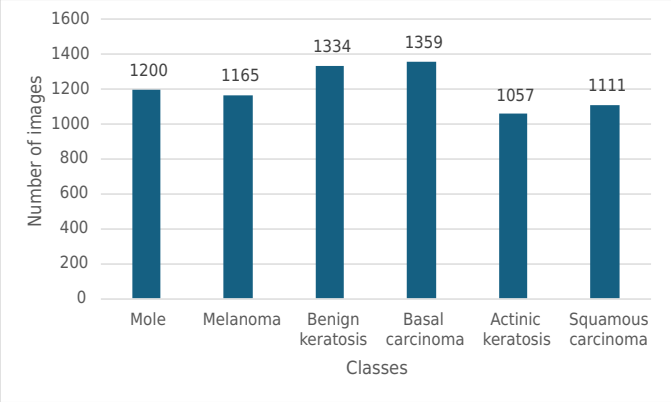

Fig. 1.3 Histogram of distribution by class after SMOTE

1.2.3 Convolutional neural network design

Four convolutional neural network architectures were evaluated: Xception [35], Resnet152V2 [36], EfficientnetV2 [37] and MobilenetV2 [38]. Each of these was loaded from the Keras library with the weights predefined by imagenet [39], subsequently the last default classification layer was removed and the option to train the weights of the convolutional layers was enabled.
To perform the training, a "GlobalAveragePooling" layer was added to reduce the convolution output and at the same time generate an output vector with the features of interest. After this layer, a dense layer of six neurons with SoftMax activation function was added to classify among the 6 types of lesions of the study.

Fig. 1.4 Architecture for evaluating the design of convolutional networks

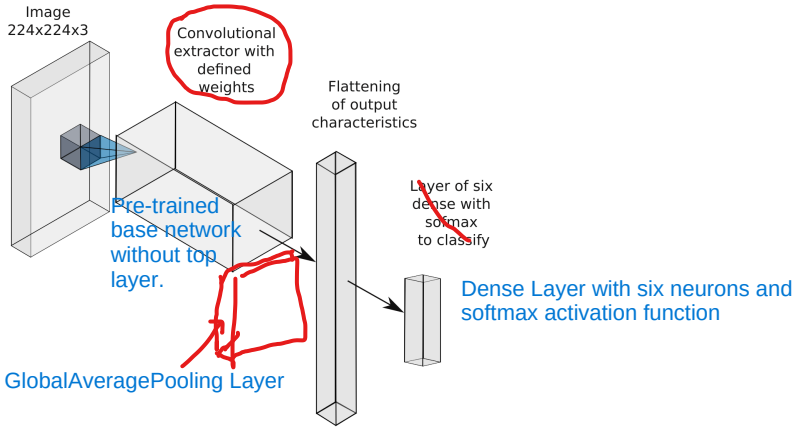

The architecture described in Figure 1.4 was trained with batch sizes of 64 images for 40 epochs at a learning rate of 0.001 with an Adam optimizer and a categorical cross-entropy loss function. In addition, a learning rate step-down function was added to stop learning and a function to stop training in case performance did not improve for 5 epochs.

After training the 4 architectures described above and evaluating their performance using the validation set, the EfficietnetV2 convolutional neural network architecture was chosen as it obtained the best performance at this stage. Once the layers were trained under the scheme described above, the classification layer was eliminated and dense layers were added to reduce the output features, these layers were sequentially counted with 1280, 1280, 640, 320, 160 neurons, with GeLU activation function; it is worth mentioning that at the end of each of these layers a DropOut layer of 0.6 was added to avoid overtraining. Finally, at the output of these dense layers, an output dense layer of 6 neurons with Softmax activation function was added again to perform the classification again. Figure 1.5 shows the architecture described above.

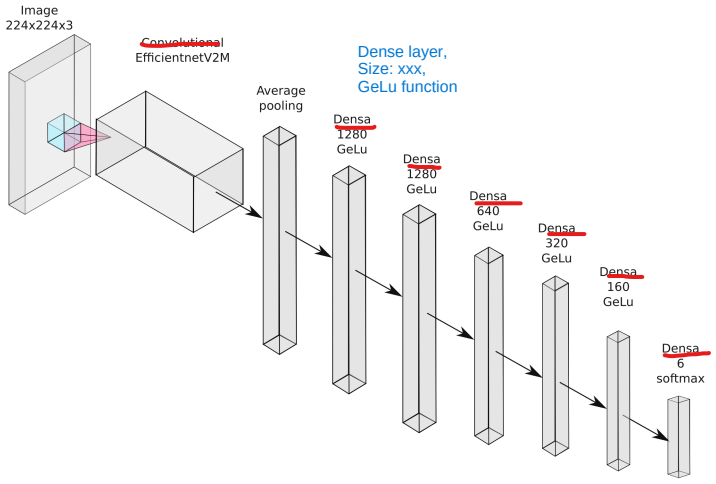

Fig. 1.5 Network architecture for sorting (each dense layer upstream of the output has DropOut of 0.6)

1.2.4 Application design

For the design of the application, Android Studio [41] was used, which, in order to interpret keras/tensorflow models, requires them to be in tensorflowlite (tflite) format [42]. This format is lightweight, encrypted in folders and designed to work in applications with low performance equipment such as a cell phone, tablet or

microcomputer. Then, the following lines of code were applied to make the change to the tensorflowlite format:

```
#Install dependency
!pip install tflite-model-maker
import tensorflow as tf

# load the model developed above
model= tf.keras.models.load_model ('path')

# define model specifications required for android #studio
converter=tf.lite.TFLiteConverter.from_keras_model (model)
converter.target_spec.supported_ops = [
  tf.lite.OpsSet.TFLITE_BUILTINS,
  tf.lite.OpsSet.SELECT_TF_OPS ]

# apply the conversion
tflite_model = converter.convert()
open("converted_model.tflite", "wb").write(tflite_model)
```

In the previously described program, it is important to highlight that the function ”tf.lite.OpsSet.TFLITE_BUILTINS” and ”tf.lite.OpsSet.SELECT_TF_OPS” allows to perform native operations of the tensorflow library, and although it adds slightly weight, it is necessary to run efficiently in the application developed in Android Studio.
The original weight of the model has a .h5 format (hierarchical data format), which contains multidimensional arrays of scientific data and had a final weight in memory of 284 MB; transforming the model to tensorflowlite format reduced the weight of this to 110.5 MB, which gave the opportunity to add more dense layers and convolution filters to the model without exceeding the 200MB limitation requested by Android studio, however no model showed improvement, so it was determined to keep the model already created for the application.
Once the interface was designed, the dependencies for the Android device and libraries required for the functionality of the system were imported and the application was installed on the mobile device. The application process is described below:
First , the application must be installed on the device, this can be done directly through Android Studio with the help of a USB cable. Once the install option is selected, the mobile device will display the message shown in Figure 1.6, asking for permission to install the software on the device.

Next, the installed application will open and the menu shown in Figure 1.7 will be displayed. The user will be presented with two options in the form of buttons to analyze an image: the first option is to acquire an image using the device’s camera, while the second will allow the user to browse its image libraries to select an image if it is preloaded.

Fig. 1.6 Installation process

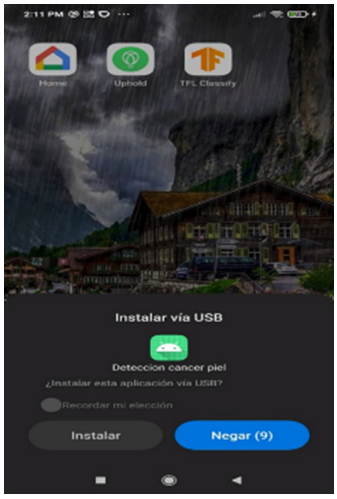

Edit the language of the figures or you must indicate that the application was made in Spanish language

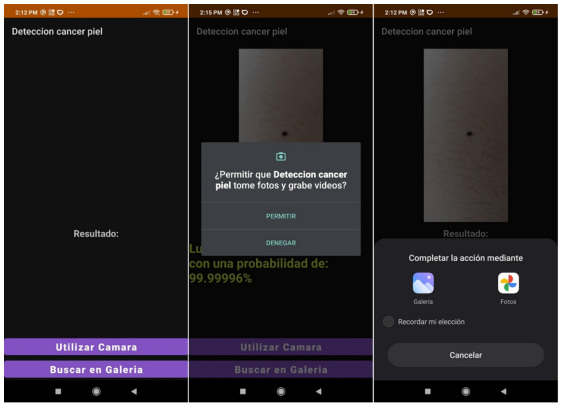

Fig. 1.7 Application menu and image selection

1.2.5 Simulation of the system

Once the image to be analyzed has been selected, a display of the selected image will be shown on the main screen and the classification given by the model will be shown below it, together with the probability of this classification with respect to the rest of the 6 classes that can be evaluated. The display of results in the application is shown below in Figure 1.8. It should be noted that in this figure a real evaluation was performed with a test subject who is sure to have had this mark since birth, so it is indeed a mole.

Fig. 1.8 Display of results

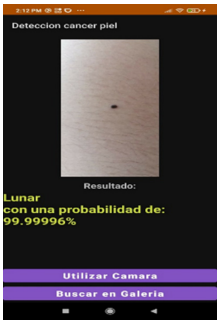

Edit the language of the figures

1.3 Results

Two experiments were carried out, the first one training the networks with the original images and later with the set that had the images added with the SMOTE balancing of the dermatofibroma class. The training was performed with 100 epochs using a function that decreases the learning rate gradually and another function that stops the training at the moment when the loss metric monitored in the validation set stops converging, this to avoid overfitting to the training data. The results during the training process are shown in Figure 1.9 and 1.10.

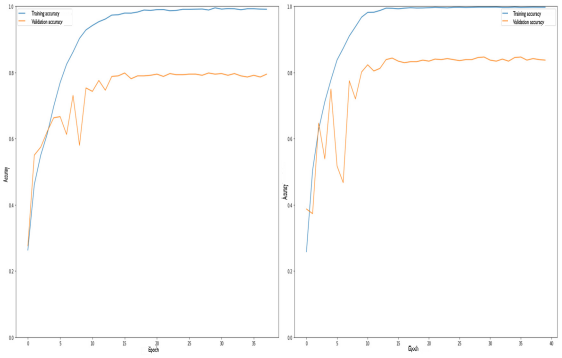

Fig. 1.9 Accuracy results without SMOTE (left), with SMOTE (right)

Subsequently, an evaluation was carried out with the final model using the data initially reserved for testing, which did not contain artificial images. To perform this evaluation, a confusion matrix was constructed, the result of which is shown in Figure 1.11.

To analyze the performance of accuracy, sensitivity and F1-score for each of the classes, a ranking report was made, as shown in Table 1.4.

In addition, ROC (Receiver Operating Characteristic) curves [40], which is a graphical representation of the sensitivity (ratio of true positives) versus the pro-

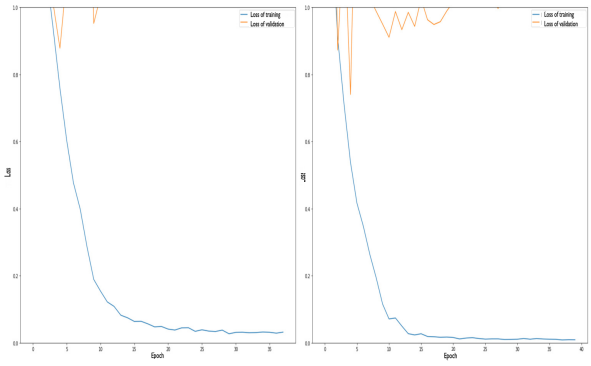

Fig. 1.10 Loss results without SMOTE (left), with SMOTE (right)

Fig. 1.11 Validation confusion matrix

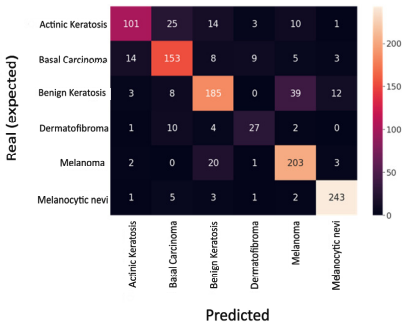

Table 1.4 Classification report by category

Class	Precision (%)	Sensitivity (%)	F1-score (%)	Number of Images
Actinic keratosis	83	66	73	154
Basal carcinoma	76	80	78	192
Benign keratosis	79	75	77	247
Dermatofibroma	66	61	64	44
Melanocytic nevi	93	95	94	255
Accuracy (%)			83	1121

portion or ratio of false positives (1-specificity) for a binary classifier system as the discrimination threshold (value at which it is decided that a case is a positive) is varied [34], were also used for the evaluation. The results of the proposed classifier including the values of the area under the ROC curve can be seen in Figure 1.12.

Overall global accuracy performance was 73% without SMOTE and 83% with SMOTE, representing a 10% improvement overall. It can be concluded from the ROC plots that there is an AUC greater than 92% in each of the classes.

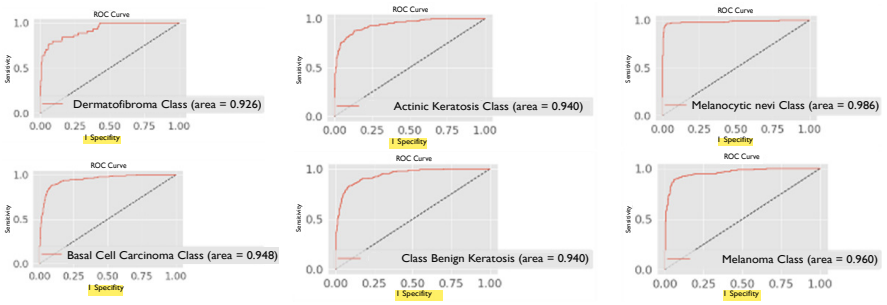

Fig. 1.12 ROC curve plots for the classification of the different classes of lesions without SMOTE

As an experiment, the app was evaluated by taking images that are not in the database, taking the image with the cell phone pointing to the computer screen, where a validated sample of each of the classes was presented, the result is shown in Figure 1.13.

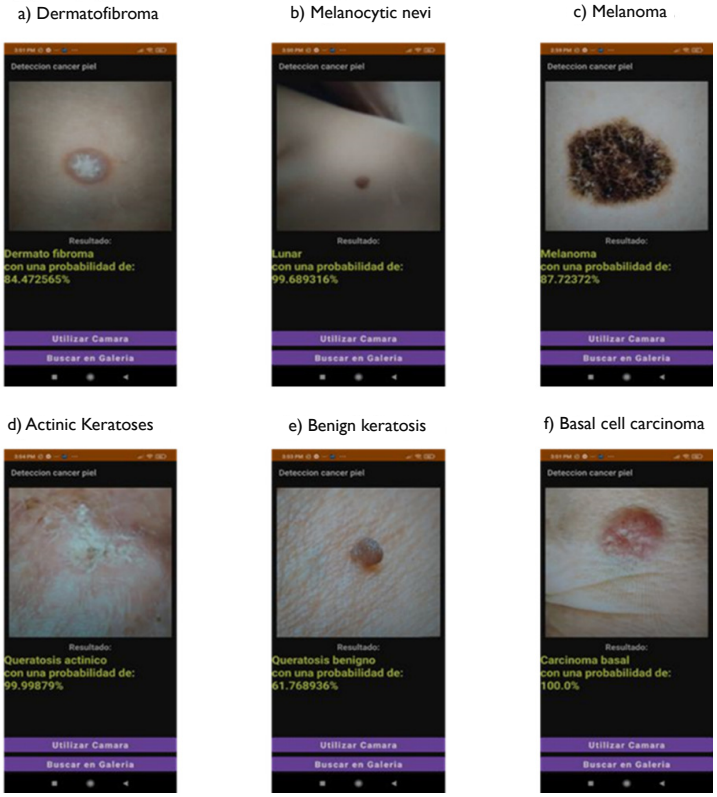

Fig. 1.13 App test with images outside the databases, taken on the computer screen

Figure 1.13 showed an effective classification response in new data, especially considering that all the evaluations except item ”d” were correct at the first attempt with low resolution images without requiring any equipment other than the cell phone. In the case of item ”d” the correct answer was obtained until the second attempt and this may be due to the fact that the first image evaluated for this case presented other figures such as hair and part of an eye, this result is shown in Figure 1.14.

Fig. 1.14 Erroneous evaluation at the first attempt, inciting basal carcinoma, actually being actinic keratosis

The average response time when introducing an image to the model in the application is 2.35 seconds, the image acquisition time is 6.58 seconds so that on average an express analysis took an average time of 9.33 seconds.

1.4 Conclusions

SMOTE balancing proved to be a great tool to generate artificial data when there is a scarce amount of data. It was demonstrated that this technique promotes a higher convergence speed when training, in spite of having a higher variance in the training. It was possible to improve the overall performance global accuracy of 73% without SMOTE and 83% with SMOTE, representing an improvement of 10% in general, in addition, it can be concluded from the ROC graphs that there is an AUC greater than 92% in all classes.

It was possible to create a low weight model (284MB) and transform it to tensorflowlite format to be applicable to an Android cellular device, reducing its weight to 110.5MB, which showed compatibility and fast response.

We were able to develop an on-device application with a simple interface that allows classifying between six different skin marks using the cell phone camera, as well as images found in the data gallery, which shows a great response in synthetic

data and real cases of moles in the test subject mentioned in the limitations section. The application demonstrated an average latency or reaction time of 9.33 seconds.

Overall accuracy results of 83% were achieved with validation data, which surpasses Dai Xaingfeng's first approach (accuracy of 72.4%) [17]. The proposed model competes with the application developed by Kousis et al. [33] (91.1% accuracy) for two classes of lesions classified as benign or malignant.; as well as with the approach using a 3D curvature pattern highlighting and convolution technique for melanoma diagnosis 89.2% accuracy by Yu Zhou [43], which requires photometric stereo equipment for its operation. Finally, it is comparable to the model proposed by B. Krohling, et al. [20], based on convolutional networks with evolutionary algorithms making use of data in the patient file, which achieved a final accuracy of 89%.

It is important to mention that all the previously mentioned works are only to evaluate the melanoma class in a binary way (positive/negative), while this work presents a solution to classify six different classes, where an F1-score of 83% was achieved in the melanoma class, with a sensitivity of 89%; at the same time the system showed an F1-Score of 94% to identify moles with a sensitivity reaching 95%. It is important to mention the area of opportunity that exists to increase the performance of the model for the identification of the rest of the lesions, whose accuracy values were low, as in the case of dermatofibroma in which only 66% was reached. One way is to explore other neural network architectures and/or models that allow the extraction of relevant features from the images together with the use of other types of classifiers. We were able to develop a cell phone application capable of classifying skin cancer images with a model based on a convolutional architecture; this model achieved an overall accuracy of 83% with test data.

References

1. N. V Chawla, K. W. Bowyer, L. O. Hall, and W. P. Kegelmeyer, "SMOTE: Synthetic Minority Over-sampling Technique," 2002.
2. C. Alonso-Belmonte, T. Montero-Vilchez, S. Arias-Santiago, and A. Buendía-Eisman, "Situación actual de la prevención del cáncer de piel: una revisión sistemática," Actas Dermosifiliogr, vol. 113, no. 8, pp. 781–791, Sep. 2022, doi: 10.1016/j.ad.2022.04.015.
3. A. Saúl, Lecciones de dermatología, 16a. Mexico: Mc Graw Hill, 2015.
4. P. C. Gameros and J. Eljure Téllez, "El cáncer de piel, un problema actual," Revista de la Facultad de Medicina de la UNAM, Ciudad de México, pp. 6–14, Jan. 11, 2016.
5. A. Cámara-Salazar et al., "Características individuales y por entidad federativa de la mortalidad por melanoma en México entre 2014 y 2018," Dermatol Rev Mex, pp. 248–254, May 2020
6. R. Roldan, "Cáncer de piel, el segundo más frecuente en México, advierte investigador de la UNAM," UNAM, 2017. [Online]. Available via DIALOG.: https://www.dgcs.unam.mx/boletin/bdboletin/2017_237.html. Cited 18 Oct 2020
7. R. R. Marín and B. C. Ortega, "Criterios dermatoscópicos para el diagnóstico de lesión melanocítica y melanoma cutáneo Dermoscopic criteria for the diagnosis of melanocytic lesions and cutaneouos melanoma," Dermatología Cosmética, Médica y Quirúrgica, pp. 142–148, 2014.
8. A. P. Kassianos, J. D. Emery, P. Murchie, and F. M. Walter, "Smartphone applications for melanoma detection by community, patient and generalist clinician users: A review," British Journal of Dermatology, vol. 172, no. 6, pp. 1507–1518, Jun. 2015, doi: 10.1111/bjd.13665.

9. M. A. Al-Asadi and A. Altun, "Deep learning with SMOTE techniques for improved skin lesion classification on unbalanced data," Selcuk University Journal of Engineering Sciences, vol. 21, no. 03, pp. 97–104, 2022
10. O. O. Abayomi-Alli, R. Damaševičius, S. Misra, R. Maskeliūnas, and A. Abayomi-Alli, "Malignant skin melanoma detection using image augmentation by oversampling in nonlinear lower-dimensional embedding manifold," Turkish Journal of Electrical Engineering and Computer Sciences, vol. 29, pp. 2600–2614, 2021, doi: 10.3906/elk-2101-133.
11. C. C. Chang, Y. Z. Li, H. C. Wu, and M. H. Tseng, "Melanoma Detection Using XGB Classifier Combined with Feature Extraction and K-Means SMOTE Techniques," Diagnostics, vol. 12, no. 7, Jul. 2022, doi: 10.3390/diagnostics12071747.
12. X. Tong, J. Wei, B. Sun, S. Su, Z. Zuo, and P. Wu, "Ascu-net: Attention gate, spatial and channel attention u-net for skin lesion segmentation," Diagnostics, vol. 11, no. 3, Mar. 2021, doi: 10.3390/diagnostics11030501.
13. K. Shehzad et al., "A Deep-Ensemble-Learning-Based Approach for Skin Cancer Diagnosis," Electronics 2023, Vol. 12, Page 1342, vol. 12, no. 6, p. 1342, Mar. 2023, doi: 10.3390/ELECTRONICS12061342.
14. S. M. Thomas, J. G. Lefevre, G. Baxter, and N. A. Hamilton, "Interpretable deep learning systems for multi-class segmentation and classification of non-melanoma skin cancer," Med Image Anal, vol. 68, Feb. 2021, doi: 10.1016/j.media.2020.101915.
15. S. Jinnai, N. Yamazaki, Y. Hirano, Y. Sugawara, Y. Ohe, and R. Hamamoto, "The development of a skin cancer classification system for pigmented skin lesions using deep learning," Biomolecules, vol. 10, no. 8, pp. 1–13, Aug. 2020, doi: 10.3390/biom10081123.
16. M. Vidya and M. V Karky, "Skin Cancer Detection using Machine Learning Techniques," IEEE International Conference on Electronics, Computing and Communication Technologies (CONECCT)CONNECT, pp. 1–5, 2020.
17. X. Dai, I. Spasić, B. Meyer, S. Chapman, and F. Andres, "Machine Learning on Mobile: An On-device Inference App for Skin Cancer Detection," 2019 Fourth International Conference on Fog and Mobile Edge Computing (FMEC), pp. 301–305, 2019.
18. P. Tschandl, C. Rosendahl, and H. Kittler, "Data descriptor: The HAM10000 dataset, a large collection of multi-source dermatoscopic images of common pigmented skin lesions," Sci Data, vol. 5, pp. 1–9, 2018, doi: 10.1038/sdata.2018.161.
19. P. Castro, B. Krohling, A. G. Pacheco, and R. A. Pacheco, "An app to detect melanoma using deep learning: An approach to handle imbalanced data based on evolutionary algorithms," in In 2020 International Joint Conference on Neural Networks (IJCNN) , IEEE, 2020, pp. 1–6.
20. A. G. C. Pacheco and R. A. Krohling, "The impact of patient clinical information on automated skin cancer detection," Comput Biol Med, vol. 116, Jan. 2020, doi: 10.1016/j.compbiomed.2019.103545.
21. R. Gao, J. Peng, L. Nguyen, Y. Liang, S. Thng, and Z. Lin, "Classification of Non-tumorous Facial Pigmentation Disorders Using Deep Learning and SMOTE."
22. S. Guo, Y. Liu, R. Chen, X. Sun, and X. Wang, "Improved SMOTE Algorithm to Deal with Imbalanced Activity Classes in Smart Homes," Neural Process Lett, vol. 50, no. 2, pp. 1503–1526, Oct. 2019, doi: 10.1007/s11063-018-9940-3.
23. IARC, "Melanoma Awareness Month 2022 – IARC." [Online]. Available via DIALOG: https://www.iarc.who.int/news-events/melanoma-awareness-month-2022/ Cited 17 Oct 2022
24. J. Bobulski and M. Kubanek, "Big data system for medical images analysis," in Frontiers in Artificial Intelligence and Applications, IOS Press BV, Dec. 2020, pp. 71–79. doi: 10.3233/FAIA200768.
25. L. Saba et al., "The present and future of deep learning in radiology," European Journal of Radiology, vol. 114. Elsevier Ireland Ltd, pp. 14–24, May 01, 2019. doi: 10.1016/j.ejrad.2019.02.038.
26. M. M. Mijwil et al., "View of From Pixels to Diagnoses Deep Learning's Impact on Medical Image Processing-A Survey," Wasit Journal of Computer and Mathematics Science, vol. 2, no. 3, pp. 9–15, 2023.

27. S. Dash, S. K. Shakyawar, M. Sharma, and S. Kaushik, “Big data in healthcare: management, analysis and future prospects,” J Big Data, vol. 6, no. 1, Dec. 2019, doi: 10.1186/s40537-019-0217-0.
28. A. Adegun and S. Viriri, “Deep learning techniques for skin lesion analysis and melanoma cancer detection: a survey of state-of-the-art,” Artif Intell Rev, vol. 54, no. 2, pp. 811–841, Feb. 2021, doi: 10.1007/s10462-020-09865-y.
29. H. P. Chan, L. M. Hadjiiski, and R. K. Samala, “Computer-aided diagnosis in the era of deep learning,” in Medical Physics, John Wiley and Sons Ltd, Jun. 2020, pp. e218–e227. doi: 10.1002/mp.13764.
30. T. Kränke, K. Tripolt-Droschl, L. Röd, R. Hofmann-Wellenhof, M. Koppitz, and M. Tripolt, “New AI-algorithms on smartphones to detect skin cancer in a clinical setting—A validation study,” PLoS One, vol. 18, no. 2 February, Feb. 2023, doi: 10.1371/journal.pone.0280670.
31. C. A. HARTANTO and A. WIBOWO, “Development of Mobile Skin Cancer Detection using Faster R-CNN and MobileNet v2 Model,” in En 2020 7th International Conference on Information Technology, Computer, and Electrical Engineering (ICITACEE). IEEE, 2020, pp. 58–63.
32. J. O. Emuoyibofarhe, D. Ajisafe, R. S. Babatunde, and M. Christoph, “Early Skin Cancer Detection Using Deep Convolutional Neural Networks on Mobile Smartphone,” International Journal of Information Engineering and Electronic Business, vol. 12, no. 2, pp. 21–27, Apr. 2020, doi: 10.5815/ijieeb.2020.02.04.
33. I. Kousis, I. Perikos, I. Hatzilygeroudis, and M. Virvou, “Deep Learning Methods for Accurate Skin Cancer Recognition and Mobile Application,” Electronics (Switzerland), vol. 11, no. 9, May 2022, doi: 10.3390/electronics11091294.
34. J. Brownlee, ”SMOTE for Imbalanced Classification with Python,” Machine Learning Mastery, [Online]. Available via DIALOG: https://machinelearningmastery.com/smote-oversampling-for-imbalanced-classification/. Cited 17 Mar 2021
35. F. Chollet, ”Xception: Deep learning with depthwise separable convolutions,” in Proceedings of the IEEE Conference on Computer Vision and Pattern Recognition, 2017, pp. 1251-1258.
36. K. He, X. Zhang, S. Ren and J. Sun, ”Deep Residual Learning for Image Recognition,” 2016 IEEE Conference on Computer Vision and Pattern Recognition (CVPR), 2016, pp. 770-778, doi: 10.1109/CVPR.2016.90.
37. B. Koonce and B. E. Koonce, Convolutional Neural Networks with Swift for TensorFlow: Image Recognition and Dataset Categorization, New York, NY, USA: Apress, 2021, pp. 109-123.
38. Sinha, D., El-Sharkawy, M. (2019). Thin mobilenet: An enhanced mobilenet architecture. In 2019 IEEE 10th annual ubiquitous computing, electronics mobile communication conference (UEMCON). IEEE, 3, 0280-0285.
39. M. A. Morid, A. Borjali, and G. Del Fiol, ”A scoping review of transfer learning research on medical image analysis using ImageNet,” Computers in Biology and Medicine, vol. 128, 2021, Art. no. 104115.
40. J. A. Swets, Signal Detection Theory and ROC Analysis in Psychology and Diagnostics: Collected Papers, 1996.
41. A. Studio, ”Android Studio: The Official IDE for Android,” 2017. [Online]. Available: https://developer.android.com/studio/. [Accessed: Jun. 24, 2019].
42. S. Li, ”TensorFlow Lite: On-device machine learning framework,” Journal of Computer Research and Development, vol. 57, 2020, p. 1839.
43. Y. Zhou, M. Smith, L. Smith, A. Farooq, and R. Warr, ”Enhanced 3D curvature pattern and melanoma diagnosis,” Computerized Medical Imaging and Graphics, vol. 35, no. 2, pp. 155-165, 2011.